PAPER

A nano continuous variable transmission system from nanotubes

IOP Publishing Nanotechnology
Nanotechnology 29 (2018) 075707 (8pp) https://doi.org/10.1088/1361-6528/aaa286

A nano continuous variable transmission system from nanotubes

Kun Cai[1,4], Jiao Shi[1], Yi Min Xie[2] and Qing H Qin[3,4]

[1] College of Water Resources and Architectural Engineering, Northwest A&F University, Yangling 712100, People's Republic of China
[2] Centre for Innovative Structures and Materials, School of Engineering, RMIT University, Melbourne 3001, Australia
[3] Research School of Engineering, Australian National University, ACT 2601, Australia

E-mail: kuncai99@163.com and qinghua.qin@anu.edu.au

Received 15 October 2017, revised 7 December 2017
Accepted for publication 18 December 2017
Published 15 January 2018

Abstract

A nano continuous variable transmission (nano-CVT) system is proposed by means of carbon nanotubes (CNTs). The dynamic behavior of the CNT-based nanosystem is assessed using molecular dynamics simulations. The system contains a rotary CNT-motor and a CNT-bearing. The tube axes of the nanomotor and the rotor in the bearing are laid in parallel, and the distance between them is known as the eccentricity of the rotor with a diameter of d. By changing the eccentricity (e) of the rotor from 0 to d, some interesting rotation transmission phenomena are discovered, whose procedures can be used to design various nanodevices. This might include the failure of rotation transmission—i.e. the rotor has no rotation—when $e \geqslant d$ at an extremely low temperature, or when the edges of the two tubes are orthogonal at their intersections in any condition. This hints that the state of the nanosystem can be used as an on/off switch or breaker. For a system with $e = d$ and a high temperature, the rotor rotates in the reverse direction of the motor. This means that the output signal (rotation) is the reverse of the input signal. When changing the eccentricity from 0 to d continuously, the output signal gradually decreases from a positive value to a negative value; as a result a nano-CVT system is obtained.

Supplementary material for this article is available online

Keywords: carbon nanotube, continuous variable transmission, nanomachine

(Some figures may appear in colour only in the online journal)

1. Introduction

In a rotary nanodevice, such as a nanomotor or a nano-bearing system, the friction between the shaft and the bearing should be made as small as possible to reduce energy dissipation. Meanwhile, the strength of the components in a nanodevice should be strong enough for the the system to be stable. CNTs can meet the requirements above due to the ultra-low friction between two neighboring concentric tubes [1–4] and extremely high in-shell strength [5–7]. Making use of this advantage, Fennimore *et al* [8] and Bourlon *et al* [9] built a rotary micromotor in which the CNTs acted as a shaft attached blades, where the charged blade can be actuated to rotate in an external electric field. Barreiro *et al* [10] found that a cargo attached to the outer tube can be driven to move on a long CNT which has an axial temperature gradient. Obviously, the dimensions of the devices above are about 100 nm. Hence, CNT components must be available in devices with sizes in the nanoscale. However, the fabrication of nanodevices with sizes of about 10 nm is still challenging in the laboratory. Molecular dynamics (MD) simulation approaches thus need to be employed to predict or estimate the dynamic response of the devices in the design process. For instance, MD methods are widely used in the design of rotary nanomotors [11]. Kang and Hwang [11] investigated a nanoscale engine composed of a carbon nanotube oscillator,

[4] Authors to whom any correspondence should be addressed.

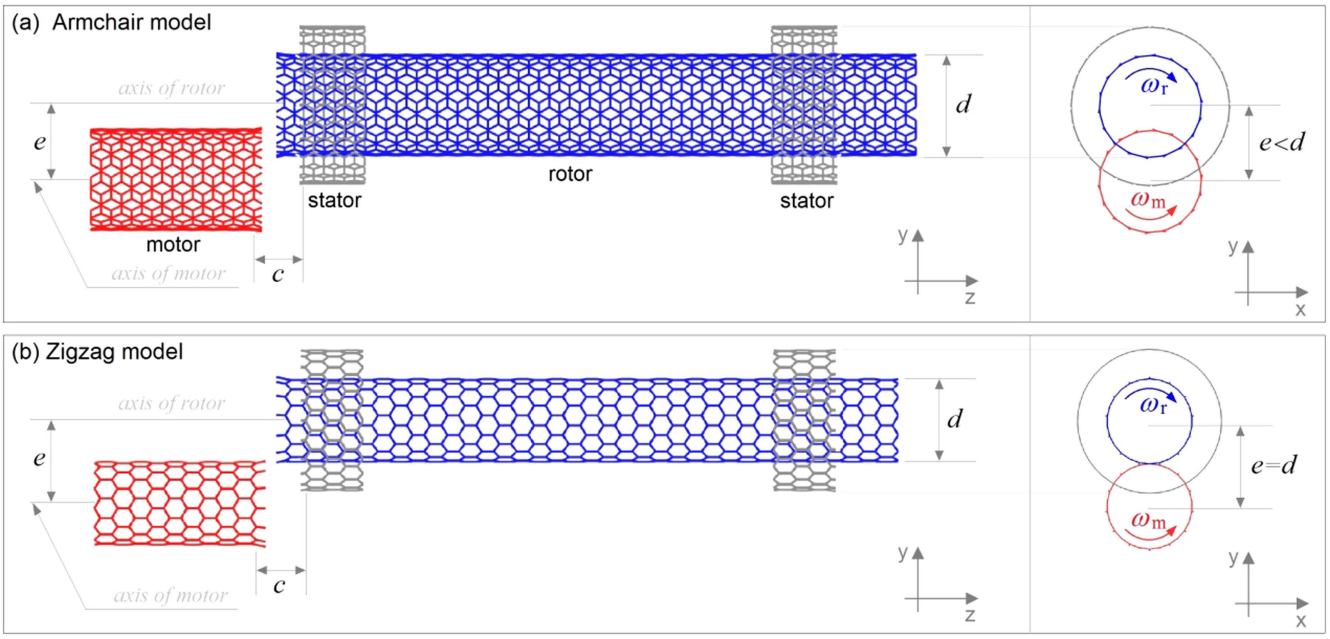

Figure 1. Schematic models of the nano continuous variable transmission (nano-CVT) CNT systems. The nanosystem is made from (a) armchair CNTs and (b) zigzag CNTs. In each nanosystem, there is a short red tube acting as a motor with a constant input rotational frequency of ω_m, and a long blue tube as a rotor with an output rotational frequency of ω_r. The rotor with a diameter of d is constrained by two short stators (gray tubes). The eccentricity of the rotor with respect to the motor is labeled as 'e'. The axial distance between the right edge of the motor and the left edge of stator is labeled as 'c'. The value of c may change slightly during rotation transmission. All atoms on the gray tubes are fixed during simulation. The neighboring edges of tubes are hydrogenated; more details of the models are listed in table 1.

motor, channel, nozzle, etc. The nanomotor was driven to rotate by nanofluid. Based on the Smoluchowski–Feynman ratchet, Tu and Hu presented a rotary nanomotor from a long inner CNT and a short outer CNT [12]. The chiral outer tube can be actuated to rotate on the inner tube, which has a varying electrical voltage along the tube axis. Wang *et al* [13] proposed a rotary nanomotor, in which the blades are driven to rotate in an external electric field when they periodically charge and discharge. Cai *et al* [14–16] developed and modified the thermally driven rotary nanomotor model from concentric CNTs.

In a rotary nanomachine [17, 18], the rotation of the rotor in the nanoengine may not be used directly. Similar to the gear-box in a car, which transforms the input rotation from the engine to the output rotation of the wheels, Cai *et al* [19] presented a CNT rotation transmission nanosystem. They also found that the over-speeding transmission of a curved nano-bearing can be used as a nano universal joint [20, 21]. Via the curved nano-bearing, both the direction and the magnitude of the output rotation are different from those of the input rotation. However, the curved angle of the nano-bearing is limited to be far less than 180°, at which angle the rotor may rotate in the opposite direction to the motor.

Like the continuous variable transmission (CVT) in a car, which continuously adjusts the input rotation into different output rotation, in the present study we proposed a nano-CVT model with a CNT-based parallel-axis rotation transmission system. In the model, the axes of the nanomotor and the rotor in the nano-bearing are parallel, rather than always collinear. Through the edge interaction at their adjacent ends, the input rotation of the nanomotor will be transformed into a different output rotation which depends on the distance between their axes. MD simulations are carried out to show the detailed response of the transmission effect in different conditions.

2. Models and methodology

2.1. Models

Figure 1 displays the schematics of the two models for RTS. The eccentricity of the rotor may not be zero during fabrication. To show the effect of the eccentricity of the rotor on its output rotation, eccentricities of 0, 0.1d, 0.5d and d are considered. Besides the eccentricity, two other factors are also studied in the simulation. One is the input rotational frequency ω_m of the motor; this is assumed to be 50, 100, 200 and 250 GHz, respectively. Another is the temperature of the system in a canonical ensemble; in the simulation, the temperature is set to be 8 K, 150 K, 300 K and 500 K, respectively.

2.2. Methodology

The dynamics of the system is investigated using molecular dynamics simulation via the open source code LAMMPS [22]. The interactions between carbon and/or hydrogen atoms are calculated using the AIREBO potential [23]. The time-step in the time integral is set to be 0.001 ps. Each simulation contains the following major steps:

(1) Build the model with specified parameters listed in table 1;

Table 1. The parameters of the tubes in the RTS shown in figure 1. The eccentricity (e) is a variable in the simulation.

	Chirality of tubes			Carbon and hydrogen atoms in tubes			Initial geometry/nm	
Model	Motor	Rotor	Stators	Motor	Rotor	Stators	c	d
Armchair	(9, 9)	(9, 9)	(14, 14)	324C + 18H	1152C + 18H	448C + 56H	0.6	1.22
Zigzag	(13, 0)	(13, 0)	(22, 0)	286C + 13H	962C + 13H	396C + 44H	0.6	1.018

(2) Update the initial positions of atoms in the system by minimizing its potential energy;
(3) Initiate the velocities of atoms with respect to the given temperature by satisfying the Gaussian distribution;
(4) Relax the system for 100 ps. During relaxation, the carbon atoms on the two rings at the right-hand edge of the motor, the two rings at the left-hand edge of the rotor, or the whole stator are fixed;
(5) Release the fixed atoms on the rotor and motor after relaxation, and specify the input rotational frequency of the motor instantaneously. Put the rotor in a canonical (NVT) ensemble at a given temperature, using a Nosé–Hoover thermostat [24, 25] to modify it;
(6) Run the system and record the data produced;
(7) Stop for post-processing.

For the convenience of comparison, we define the ratio of rotation transmission (RRT) as

$$R = \omega_r/\omega_m. \quad (1)$$

When R is positive, the rotor has the same rotational direction as that of the motor; otherwise, the two tubes will rotate in reverse directions. In particular, when $R = 1$, the rotor rotates synchronously with the motor. If $R = 0$, the rotor's rotational speed equals zero on time average.

It should be mentioned that the dynamic behavior of the rotor depends on two interactions. One is the interaction between the motor and the rotor via the vdW effect at the adjacent edges [26]; for simplicity, we call it edge interaction. The other is the interaction between the rotor and the stators, which is called inter-shell interaction and is caused by potential barriers on the tubes [27, 28]. The acceleration of a rotor means that the edge interaction is stronger than the inter-shell interaction. If the rotor is in a stable rotation, the two interactions are in equilibrium.

3. Numerical simulation and discussion

3.1. Eccentricity effect

As the axes of the motor and the rotor of the RTS shown in figure 1 are not collinear, the interaction between their adjacent edges is not as strong as that between the two co-axial tubes. It is confirmed from figure 2 that the stable value of R decreases with an increase in the eccentricity of the rotor in the armchair model. The maximum of R is achieved when there is no eccentricity, i.e. $e = 0d$. If the rotor has a small eccentricity, i.e. $e = 0.1d$, the rotor rotates synchronously with the motor within the first 5 ns; however, the rotation transmission is not as stable as in the case of $e = 0d$. For example, between 7 ~ 8 ns in the red curve in figure 2(a) with respect to 50 GHz of rotational frequency input, the value of R is less than 1.0. If the eccentricity of the rotor is larger, e.g. $e = 0.5d$, the stable value of R is ~0.3.

If the eccentricity of the rotor reaches $1.0d$, i.e. the two tubes are externally tangential, the value of R is ~−0.6. The negative value of R represents the rotor rotating in the reverse direction of the motor. Compared to a macro gear train in which $R = -1.0$ due to the same radii of the two externally tangential gears, the rotation transmission of the two nanotubes via the interaction of their adjacent edges is weaker. The reason for this is that the inter-shell friction increases with the relative sliding speed [4, 29, 30]. When $\omega_r = -0.6\omega_m$, the inter-shell friction balances the edge interaction. If ω_r grows larger, the friction will be greater than the edge interaction causing the negative acceleration of the rotor, and further leading to a decrease of ω_r.

From the stable values of R shown in figure 2, we know that the rotational direction of the rotor varies with the value of its eccentricity. For example, the rotor has the same rotational direction as the motor when $e \leqslant 0.5d$ and $\omega_m = 100$ GHz (movie 1 is available online at stacks.iop.org/NANO/29/075707/mmedia). If $e = 1.0d$, the rotor rotates in a reverse direction to the motor (movie 2). This means that the rotational direction of the rotor can be adjusted to meet the practical needs by changing the eccentricity of the rotor.

When the input rotational frequency becomes higher, the stable R values of the rotors vary with the eccentricity as well. For instance, the value of R is about 0.8 when $\omega_m = 100$ GHz and $e = 0.1d$ (figure 2(b)), or ~0.76 when $\omega_m = 250$ GHz. When driven by a high-speed motor, e.g. $\omega_m = 200$ or 250 GHz (figures 2(c) and (d)), the R value of the rotor becomes less than 1.0 relative to the system without eccentricity. This is due to the larger amount of friction between the rotor and stators when the input rotational frequency is larger [19, 31].

Comparing the R values of the rotor with $e = 0.5d$ and $1.0d$ when driven by the motor with different values of ω_m, the absolute value of R corresponding to $\omega_m = 200$ GHz is maximum among the four cases. This implies that the vdW interaction between the adjacent edges of the motor and rotor has a maximum value when the relative sliding speed increases continuously.

In the analysis above, the nanosystem is formed with armchair CNTs. As we know, a potential barrier on the surface of an armchair CNT goes along the generatrix [27]. Inter-shell friction is mainly caused by the interaction of the potential barriers. Hence, the rotation of the rotor can only be successfully excited when the edge interaction is greater than

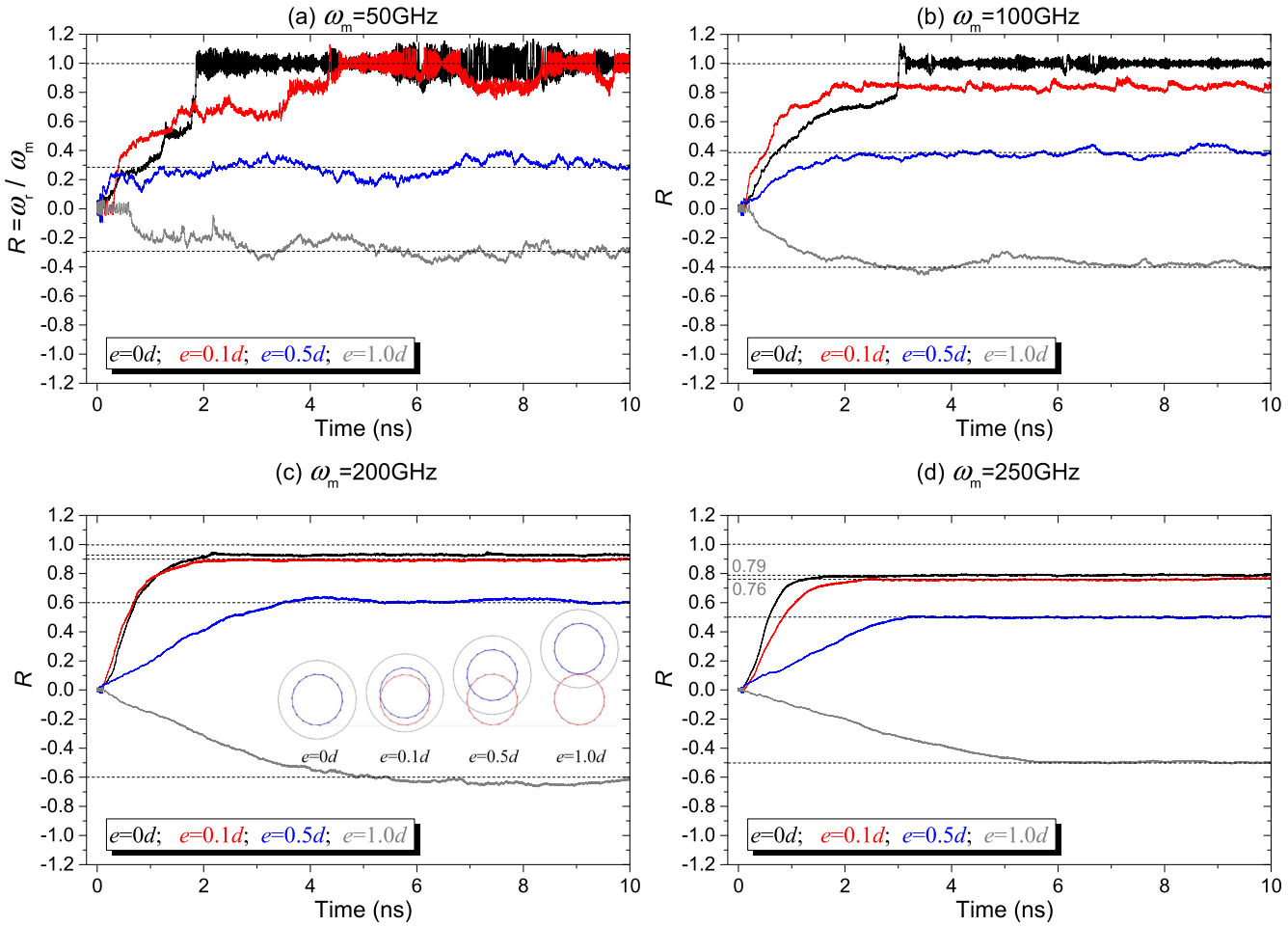

Figure 2. The RRT histories of the rotors with different eccentricities driven by the motor with different input rotation in the armchair model at 300 K. The inset in (c) shows the configurations of the system with different eccentricities in the *xy* plane. The black curves correspond to the '$e = 0d$' case, the red curves to the '$e = 0.1d$' case, the blue curves to the '$e = 0.5d$' case and the light gray curves to the '$e = 1.0d$' case. The same behind.

the inter-shell friction. Unlike the armchair tube, a zigzag CNT has potential barriers located in the cross-sections of the tube. Hence, the inter-shell friction between the two concentric zigzag CNTs should be smaller than that between two armchair tubes if they have the same geometry and the same environment. Hence, the rotor should behave differently.

Figure 3 gives the histories of the RRT of the zigzag rotors during simulation in different conditions. For instance, when $\omega_m = 50$ GHz, the rotor is actuated to rotate synchronously with the motor, i.e. $R = 1.0$, within 0.5 ns, rather than 5 ns for the armchair rotor. Hence, the edge interaction mainly determines the acceleration of the rotor due to the slight inter-shell friction. If the rotor has any eccentricity, the rotor does not rotate synchronously with the motor. In particular, when $e = 1.0d$, the rotor is not able to drive to rotation within 10 ns, which is considered as a failure of rotation transmission. This means that the edge interaction is even weaker than the inter-shell friction when the zigzag motor is externally tangential to the zigzag rotor.

However, if the input rotation frequency is larger, e.g. $\omega_m \geqslant 100$ GHz, the rotor will be driven to rotate quickly. For example, the rotor rotates synchronously with the motor within 2 ns on the condition that $\omega_m \leqslant 200$ GHz and the rotor has no eccentricity. If the rotor has small eccentricity, e.g. $e = 0.1d$, the stable value of R is smaller than 1.0. In particular, when $\omega_m = 250$ GHz and $e = 0.1d$, the stable value of R is identical to that with respect to $e = 0d$. The reason for this is that the edge atoms on the motor move closer to the rotor's edge but away from the motor's tube axis under a larger centrifugal force, which is generated by the higher rotational frequency of the motor. Furthermore, the small eccentricity is made up by the enlargement of the motor's edge at a very high rotational speed. When $e = 0.5d$, the stable R value of the zigzag rotor decreases from 0.5 to 0.34 with the increase of ω_m. The value of R is lower compared to the values of the armchair rotor shown in figure 2. Hence, edge interaction in the zigzag model is far less than that in the armchair model. If the rotor and the motor are externally tangential, i.e. $e = 1.0d$, the absolute value of R is larger than that of the rotor in the armchair model. This tells us that the edge interaction becomes stronger when the motor has a

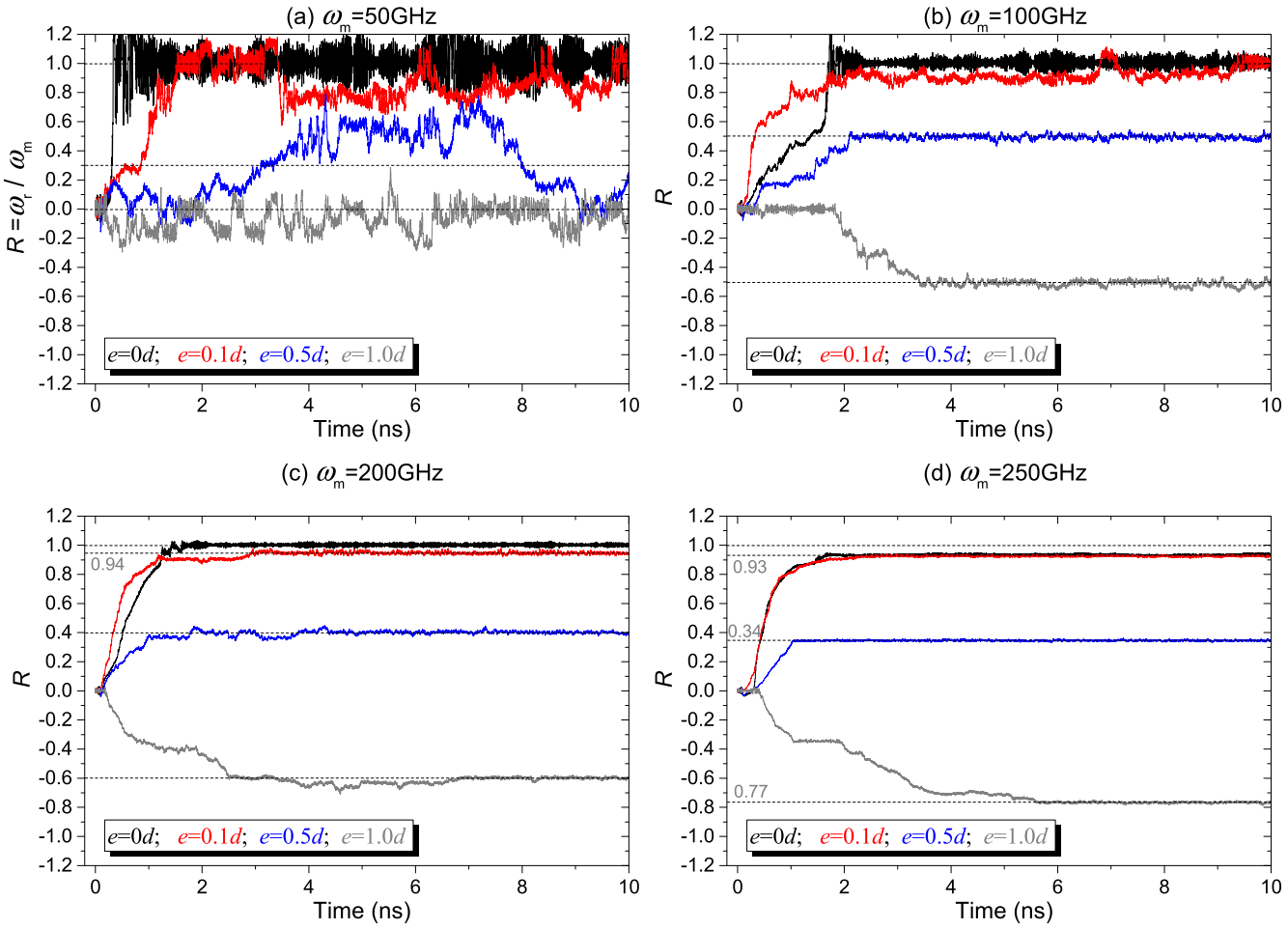

Figure 3. The RRT histories of the rotors with different eccentricities driven by the different input rotation of the motor in the zigzag model at 300 K.

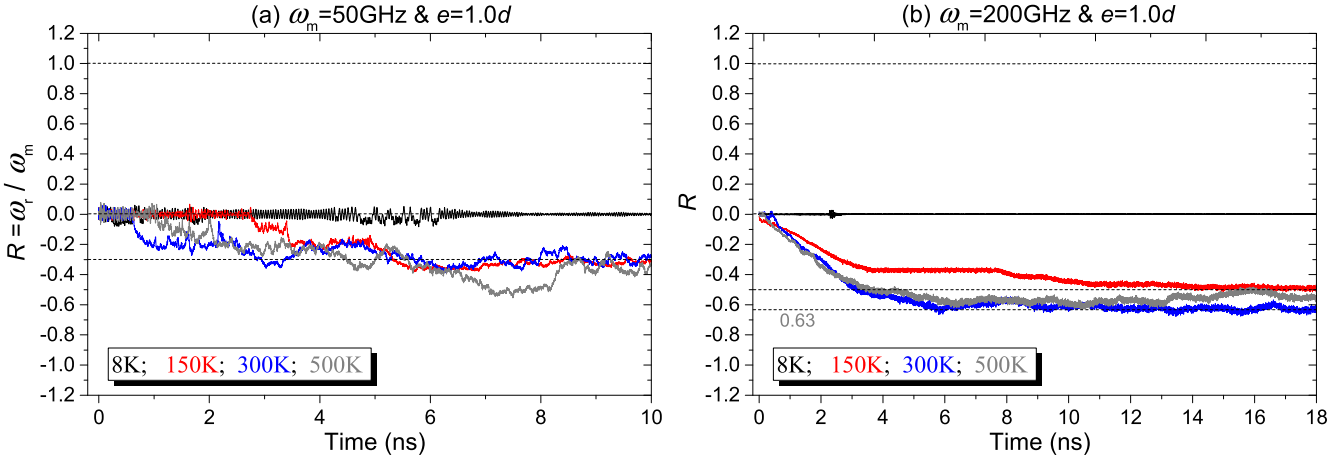

Figure 4. Histories of the R of the rotor in the armchair model with $e = 1.0d$.

larger rotational frequency, which results in the enlargement of the tube's edge at a higher centrifugal force.

3.2. Temperature effect

To show the effect of the thermal vibration of the atoms on the edge interaction, we choose a rotor with $e = 1.0d$ and a motor with 50 GHz or 200 GHz as the input rotational frequency, and expose the system to four different temperatures, i.e. 8 K (extremely low), 150 K (low), 300 K (common) and 500 K (high), respectively.

In figure 4, the rotor cannot be driven to rotate at extremely low temperatures. Both the radial and axial vibration of the edge atoms on both the motor and the rotor are

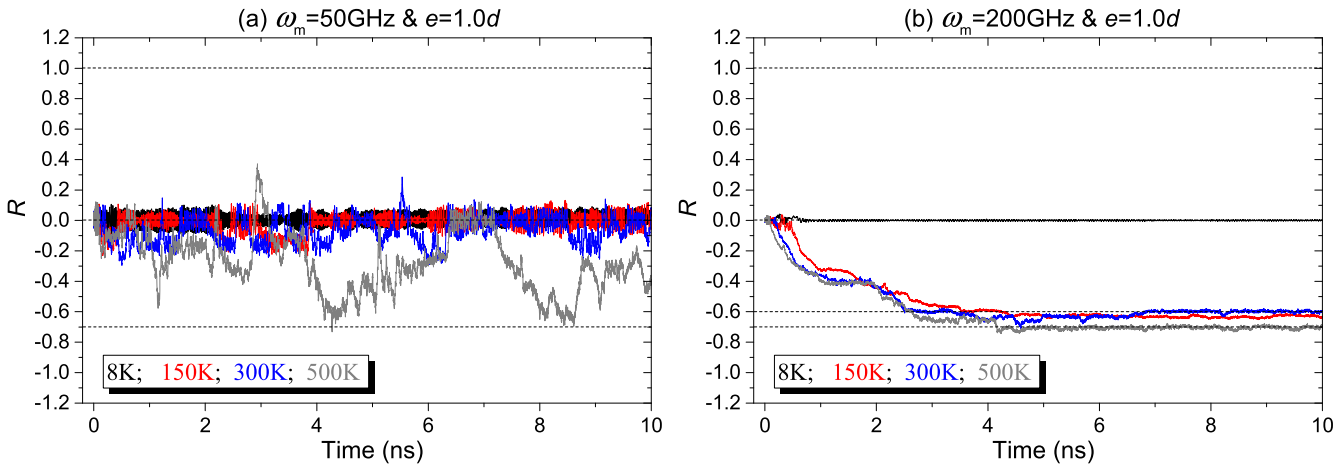

Figure 5. Histories of R of the rotor in the zigzag model with $e = 1.0d$.

significant for rotation transmission/coupling. The reason for this is that the axial vibration provides stronger interaction between the motor and the rotor at the adjacent edges, the radial vibration leads to nonuniform interaction between the adjacent edges and the circumferential component of the impulsion from the motor provides torque. Hence, at very low temperatures, a slight thermal vibration leads to failure of the rotational coupling.

However, the rotor can be driven to rotate successfully at temperatures higher than 150 K. In addition, the values of R at different temperatures have nearly the same stable value when $\omega_m = 50$ GHz (see figure 4(a)). For example, the stable values of R tend to be 0.3 when $\omega_m = 50$ GHz (figure 4(a)). If $\omega_m = 200$ GHz (figure 4(b)), the stable R values are between 0.5 and 0.63.

We also investigate the temperature effect in a zigzag model. For example, in figure 5(a), the rotor fails to rotate at any temperature when $\omega_m = 50$ GHz. However, if $\omega_m = 200$ GHz (figure 5(b)), the rotor is unable to rotate at 8 K only. If the temperature is higher than 150 K, the values of R are between 0.6 and 0.7.

From the results in figures 4 and 5, one conclusion can be made: the rotor cannot be driven to rotate at extremely low temperatures. The reason for this is that the thermal vibration amplitudes of the edge atoms on the tubes are negligible at extremely low temperatures. Hence, the edge interaction and the inter-shell friction are too weak, and the rotor cannot be driven to rotate. Actually, this implies that the rotation transmission can be controlled by regulating the temperature.

3.3. Mechanism for rotation transmission between motor and rotor

From the numerical assessment above, in general, the rotor can be driven to rotate via a period of acceleration. The acceleration process of the rotor is determined by the difference between the edge interaction and the inter-shell friction. Successful rotation transmission only happens when the edge interaction is stronger than the static friction between the rotor and the stators. Figure 6 gives the interaction between the adjacent edges of the motor and

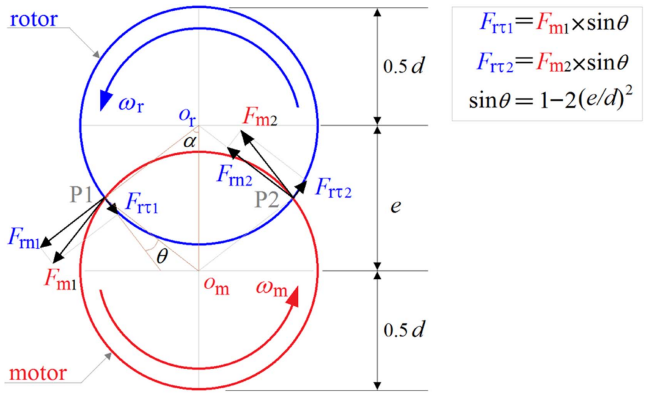

Figure 6. The ideal edge interaction between the motor and the rotor.

the rotor. In figure 6, $\boldsymbol{F}_{m1}$ and $\boldsymbol{F}_{m2}$ are the friction applied to the rotor by the motor at the contact points P1 and P2. Each force vector can be decomposed into two components, i.e. $\boldsymbol{F}_m$ being along the normal of the edge of the rotor, and $\boldsymbol{F}_{r\tau}$ along the tangent of the edge of the rotor. The normal component, $\boldsymbol{F}_m$, causes the vibration of the edges within the local cross-section and contributes nothing to the rotation transmission. However, the tangential component, $\boldsymbol{F}_{r\tau}$, will generate a moment about the tube axis, therefore leading to the angular acceleration of the rotor if the moment is larger than the resistant moment by the inter-shell friction from the stators.

On the other hand, as we consider $\boldsymbol{F}_m$ to be the velocity of the contact point on the edge of the motor, the component $\boldsymbol{F}_{r\tau}$ is the velocity of the rotor at the contact point, correspondingly. Due to the identical radius of the two tubes, the following relation reads

$$\boldsymbol{F}_{r\tau}/\boldsymbol{F}_m = (0.5d_r \times \omega_r)/(0.5d_m \times \omega_m) = R, \qquad (2)$$

where D_r and d_m are the diameters of the rotor and the motor, respectively. If the two tubes have no relative sliding at their contact points, i.e. the ideal rotation transmission, the value of R can be mathematically expressed as

$$R = 1-2(e/d)^2. \qquad (3)$$

So, we have the following results: (1) synchronous rotation happens when $e = 0d$. (2) The rotational frequency of the rotor is half that of the motor when $e = 0.5d$. (3) $R = -1$ when $e = 1.0d$, i.e. the rotor rotates in the reverse direction of the motor when $e = d$. Hence, if $e = 0.1d$, i.e. slight eccentricity, the value of R equals 0.98, which is slightly less than 1.0. From the numerical results presented above, we find that, on time average, the ideal rotation transmission depends on several parameters. For example, the ideal rotation transmission is achieved when $e = 0d$ and $\omega_m \leqslant 100$ GHz at 300 K, and $e = 0d$ and $\omega_m = 200$ GHz at 300 K for the zigzag model. If $e = 0.5d$, the ideal rotation transmission only happens ($R = 0.5$) when $\omega_m = 250$ GHz in the armchair model or $\omega_m = 100$ GHz in the zigzag model. If $e = 1.0d$, the ideal rotation transmission cannot happen at all.

From equation (3), we can also predict the failure of rotation transmission when the edges of the two tubes are orthogonal at their intersections, i.e. $e \approx 0.707d$. In general, the rotation transmission state occurs between the failed rotation transmission and ideal transmission—i.e. the absolute value of R should be less than or equal to that of R from equation (3). However, there is an exception. When $\omega_m = 200$ GHz and $e = 0.5d$ in the armchair model at 300 K (the blue line in figure 2(c)), the stable value of R is near 0.6, which is larger than the ideal value, i.e. 0.5. This means that the rotor is in an over-speeding state [21]. The reason for this could be the enlargement of the edge of the motor at high rotational frequency speed. As the diameter of the motor is larger, the value of R becomes larger according to equation (2).

4. Conclusions

A nano-CVT system has been developed by integrating a CNT-based nanomotor and a nano-bearing. In this system, the output rotation of the rotor may be different from that of the motor. This phenomenon is investigated using a molecular dynamics simulation. Based on the results obtained, some conclusions are drawn for the potential application of such a nanosystem.

(1) At 300 K, the ideal rotation transmission—in which the adjacent edges of the motor and the rotor have no relative sliding—happens when the input rotational frequency of the motor is smaller than 100 GHz and the rotor has no eccentricity.
(2) Failed rotation transmission—i.e. the rotor does not rotate—happens at extremely low temperatures or when the edges of the two tubes are orthogonal at their intersections according to the theoretical prediction. The state can be used as an on/off switch in a nanodevice.
(3) If the eccentricity of the rotor reaches $1.0d$, i.e. the two tubes are externally tangential, the value of R is negative, which means that the rotational direction of the rotor is the reverse of the motor. This means one can adjust the output rotational direction by changing the eccentricity of the rotor with respect to the motor.
(4) The rotor with an eccentricity of $1.0d$ cannot be driven to rotate at extremely low temperatures, because the slight thermal vibration of the edge atoms on the tubes produces negligible edge interaction as compared to the inter-shell static friction. This implies that the rotor can be 'frozen' at extremely low temperatures if rotation transmission is not required.

Acknowledgments

The authors are grateful for the financial support from the National Natural and Science Foundation, China (Grant Nos: 11772204; 51505388) and the National Key Research and Development Plan, China (Grant No: 2017YFC0405102).

ORCID iDs

Kun Cai https://orcid.org/0000-0001-6576-0199
Yi Min Xie https://orcid.org/0000-0001-5720-6649
Qing H Qin https://orcid.org/0000-0003-0948-784X

References

[1] Cumings J and Zettl A 2000 Low-friction nanoscale linear bearing realized from multiwall carbon nanotubes *Science* **289** 602–4
[2] Guo W, Guo Y, Gao H, Zheng Q and Zhong W 2003 Energy dissipation in gigahertz oscillators from multiwalled carbon nanotubes *Phys. Rev. Lett.* **91** 125501
[3] Zhang R, Ning Z, Zhang Y, Zheng Q, Chen Q, Xie H, Zhang Q, Qian W and Wei F 2013 Superlubricity in centimetres-long double-walled carbon nanotubes under ambient conditions *Nat. Nanotechnol.* **8** 912–6
[4] Cook E H, Buehler M J and Spakovszky Z S 2013 Mechanism of friction in rotating carbon nanotube bearings *J. Mech. Phys. Solids* **61** 652–73
[5] Qiu W, Kang Y L, Lei Z K, Qin Q H and Li Q 2009 A new theoretical model of a carbon nanotube strain sensor *Chinese Phys. Lett.* **26** 080701
[6] Qin Z, Qin Q H and Feng X Q 2008 Mechanical property of carbon nanotubes with intramolecular junctions: molecular dynamics simulations *Phys. Lett.* A **372** 6661–6
[7] Qiu W, Kang Y L, Lei Z K, Qin Q H, Li Q and Wang Q 2010 Experimental study of the Raman strain rosette based on the carbon nanotube strain sensor *J. Raman Spectrosc.* **41** 1216–20
[8] Fennimore A, Yuzvinsky T, Han W-Q, Fuhrer M, Cumings J and Zettl A 2003 Rotational actuators based on carbon nanotubes *Nature* **424** 408–10
[9] Bourlon B, Glattli D C, Miko C, Forró L and Bachtold A 2004 Carbon nanotube based bearing for rotational motions *Nano Lett.* **4** 709–12
[10] Barreiro A, Rurali R, Hernandez E R, Moser J, Pichler T, Forro L and Bachtold A 2008 Subnanometer motion of cargoes driven by thermal gradients along carbon nanotubes *Science* **320** 775–8

[11] Kang J W and Hwang H J 2004 Nanoscale carbon nanotube motor schematics and simulations for micro-electro-mechanical machines *Nanotechnology* **15** 1633–8
[12] Tu Z and Hu X 2005 Molecular motor constructed from a double-walled carbon nanotube driven by axially varying voltage *Phys. Rev.* B **72** 033404
[13] Wang B, Vuković L and Král P 2008 Nanoscale rotary motors driven by electron tunneling *Phys. Rev. Lett.* **101** 186808
[14] Cai K, Li Y, Qin Q H and Yin H 2014 Gradientless temperature-driven rotating motor from a double-walled carbon nanotube *Nanotechnology* **25** 505701
[15] Cai K, Wan J, Qin Q H and Shi J 2016 Quantitative control of a rotary carbon nanotube motor under temperature stimulus *Nanotechnology* **27** 055706
[16] Cai K, Yu J, Wan J, Yin H and Qin Q H 2016 Configuration jumps of rotor in a nanomotor from carbon nanostructures *Carbon* **101** 168–76
[17] Eelkema R, Pollard M M, Vicario J, Katsonis N, Ramon B S, Bastiaansen C W, Broer D J and Feringa B L 2006 Molecular machines: nanomotor rotates microscale objects *Nature* **440** 163–163
[18] http://nobelprize.org/nobel_prizes/chemistry/laureates/2016/press.html (Accessed: 15 June 2017)
[19] Cai K, Yin H, Wei N, Chen Z and Shi J 2015 A stable high-speed rotational transmission system based on nanotubes *Appl. Phys. Lett.* **106** 021909
[20] Cai K, Cai H, Shi J and Qin Q H 2015 A nano universal joint made from curved double-walled carbon nanotubes *Appl. Phys. Lett.* **106** 241907
[21] Cai K, Cai H, Ren L, Shi J and Qin Q H 2016 Over-speeding rotational transmission of a carbon nanotube-based bearing *J. Phys. Chem.* C **120** 5797–803
[22] Plimpton S 1995 Fast parallel algorithms for short-range molecular dynamics *J. Comp. Phys.* **117** 1–19
[23] Stuart S J, Tutein A B and Harrison J A 2000 A reactive potential for hydrocarbons with intermolecular interactions *J. Chem. Phys.* **112** 6472–86
[24] Nosé S 1984 A unified formulation of the constant temperature molecular dynamics methods *J. Chem. Phys.* **81** 511–9
[25] Hoover W G 1985 Canonical dynamics: equilibrium phase-space distributions *Phys. Rev.* A **31** 1695
[26] Guo Z, Chang T, Guo X and Gao H 2011 Thermal-induced edge barriers and forces in interlayer interaction of concentric carbon nanotubes *Phys. Rev. Lett.* **107** 105502
[27] Belikov A, Lozovik Y E, Nikolaev A and Popov A 2004 Double-wall nanotubes: classification and barriers to walls relative rotation, sliding and screwlike motion *Chem. Phys. Lett.* **385** 72–8
[28] Popov A M, Lebedeva I V, Knizhnik A A, Lozovik Y E and Potapkin B V 2013 *Ab initio* study of edge effect on relative motion of walls in carbon nanotubes *J. Chem. Phys.* **138** 024703
[29] Tangney P, Louie S G and Cohen M L 2004 Dynamic sliding friction between concentric carbon nanotubes *Phys. Rev. Lett.* **93** 065503
[30] Servantie J and Gaspard P 2003 Methods of calculation of a friction coefficient: application to nanotubes *Phys. Rev. Lett.* **91** 185503
[31] Yin H, Cai K, Wei N, Qin Q H and Shi J 2015 Study on the dynamics responses of a transmission system made from carbon nanotubes *J. Appl. Phys.* **117** 234305